# Spin Transitions Induced by Magnetic Field in Quantum Dot Molecules

Ramin M. Abolfath[1,2], and Pawel Hawrylak[1]

[1] *Institute for Microstructural Sciences, National Research Council of Canada, Ottawa, K1A 0R6, Canada*

[2] *Department of Radiation Oncology, University of Texas Southwestern Medical Center, Dallas, Texas 75390, USA*

(Dated: April 30, 2008)

We present a theoretical study of magnetic field driven spin transitions of electrons in coupled lateral quantum dot molecules. A detailed numerical study of spin phases of artificial molecules composed of two laterally coupled quantum dots with $N = 8$ electrons is presented as a function of magnetic field, Zeeman energy, and the detuning using real space Hartree-Fock Configuration Interaction (HF-CI) technique. A microscopic picture of quantum Hall ferromagnetic phases corresponding to zero and full spin polarization at filling factors $\nu = 2$ and $\nu = 1$, and ferrimagnetic phases resulting from coupling of the two dots, is presented.

## I. INTRODUCTION

The application of spin of electrons in quantum dots for generation of electron entanglement and quantum information processing in solid state devices is of current experimental[1,2,3,4,5,6,7,8,9,10,11] and theoretical interest[12,13,14,15,16,17,18]. Controlling the spin of electrons in single quantum dots by tuning the external magnetic field, the confining potential, number of electrons, and Zeeman coupling has been demonstrated[2,3,4,5,6,7]. It was shown that in strong magnetic field electrons form a spin singlet quantum Hall droplet at filling factor $\nu = 2$. Increasing the magnetic field leads to the spin-flip transitions until the spin polarized filling factor $\nu = 1$ droplet is reached.[2] Spin flips beyond the first spin flip are associated with correlated states such as spin bi-excitons, identified and observed experimentally[5]. Quantum dot molecules offer additional possibility of coupling and controlling spin transitions by tuning the tunneling barrier which controls the inter-dot coupling.[12,16,17,18,19] The recently demonstrated time dependent control of the tunneling barrier height and confining potential[6], and the quantum state of the electron spin by applying oscillating magnetic field (Rabi oscillations)[7], resulted in coherent manipulation of two electron spins in coupled quantum dot molecules. Recent experiments by Pioro-Ladriere *et al.* in Ref.3 suggested that in strong magnetic field electrons are expected to form quantum Hall droplet in each quantum dot. Edge states of each droplet can be coupled in a controlled way using barrier electrodes, and at filling factor $\nu = 2$ effectively reduce the many-electron-double dot system to a two-level molecule[3]. When populated with one electron each, one expects to have singlet-triplet transitions of two valence electrons in the background of core electrons of the spin singlet $\nu = 2$ droplets. With increasing magnetic field, transitions to higher spin polarized states are expected, with coupled quantum dots resembling artificial magnetic molecules.

In this paper, we investigate the effect of the interdot tunneling and electron-electron interactions on the evolution of total spin of electrons in a quantum dot molecule as a function of electron numbers and magnetic field.

We study the many-body effects in the spin flip transitions by incorporating systematically the inter-dot and intra-dot electron-electron Coulomb interactions using real space Hartree-Fock Configuration Interaction (HF-CI) technique. We find quantum Hall droplets with zero and full spin polarization, identified as $\nu = 2$ and $\nu = 1$ quantum Hall droplets[12], in analogy with single quantum dots and quantum Hall ferromagnets[20]. Between these two states, we find series of continuous transitions among partially spin polarized phases. These partially polarized phases correspond to spin flips. Simultaneous spin flip in each isolated dot must lead to even number of spin flips in a double dot. Recently, we have found partially spin polarized phases which correspond to odd number of spin flips[21] in a double quantum dot. In Ref. [21], we have identified these correlated states as quantum Hall *ferrimagnets*.

Coherent superposition of two single particle levels in a double well potential in a form of symmetrical and antisymmetrical states is a well known example of quantum mechanical phenomena, from coherent charge oscillation of an electron between two states localized on two protons in $H_2^+$ molecules, coherent oscillation between left handed and right handed Amino acids,[22] coherent control of Rabi oscillations of electron spin in quantum dots[7], to macroscopic quantum resonance of Cooper pairs in mesoscopic superconducting grains[23]. The quantum Hall ferrimagnetic states, or spin unbalanced phases,[24,25] are also a direct manifestation of coherent quantum mechanical tunneling and inter-dot electronic correlations. These states can be described in terms of linear combinations of spin excitons localized in left and right dots, which in turn lead to coherent spin oscillations, e.g., spin counterpart of coherent charge oscillations in $H_2^+$ molecules.

The paper is organized as follows: In section II we review the Hamiltonian of electrons confined in the lateral gated quantum dots. In section III, the computational methods of single particle configuration interaction (SP-CI) and unrestricted Hartree-Fock configuration interaction (URHF-CI) are summarized. To differentiate the spin transitions of quantum dot molecules and two isolated dots with zero inter-dot interaction, we briefly

present the spin phase diagram of single dots in section IV. The microscopic picture of spin excitations in coupled quantum dots are discussed in sections V, and VI. The interpretation of spin excitations in terms of electron-hole excitations allows us to attribute the excitations with total spin $S = 1$ and $S = 2$ as spin exciton and bi-exciton. Pairing of excitons and the formation of bi-excitons due to strong inter-dot interaction is discussed. To elucidate the quantum Hall ferrimagnetic states, the real space representation of excitons is introduced. The paper is summarized in section VII.

## II. HAMILTONIAN

We describe electrons confined in quasi-two-dimensional quantum dots in a uniform perpendicular magnetic field by the effective mass Hamiltonian

$$H = \sum_{i=1}^{N} (T_i + E_{iZ}) + \frac{e^2}{2\epsilon} \sum_{i \neq j} \frac{1}{|\vec{r}_i - \vec{r}_j|}, \qquad (1)$$

where

$$T = \frac{1}{2m^*} \left( \frac{\hbar}{i} \vec{\nabla} + \frac{e}{c} A(\vec{r}) \right)^2 + V(x, y) \qquad (2)$$

is the single electron Hamiltonian in magnetic field. Here $(\vec{r}) = (x, y)$ describes electron position, $A(\vec{r}) = \frac{1}{2} \vec{B} \times \vec{r}$ is the vector potential, $B$ is the external magnetic field, and $V(\vec{r})$ is the quantum dots confining potential. $m^*$ is the conduction-electron effective mass, $e$ is the electron charge, and $\epsilon$ is the host semiconductor dielectric constant ($\epsilon = 12.8$ in GaAs). $E_{iZ} = \frac{1}{2} g \mu_B \sigma_{iz} B$ is the Zeeman spin splitting, $g$ is the host semiconductor $g$-factor ($g = -0.44$ in GaAs), $\mu_B$ is the Bohr magneton, and $\sigma$ is the Pauli matrix. In what follows, we present the numerical results in effective atomic unit (in GaAs effective Bohr radii $a_0^* = 9.79nm$, and effective Rydberg $Ry^* = 5.93meV$).

The single particle eigenvalues ($\epsilon_i$) and eigenvectors ($\varphi_i$) are calculated by discretizing $T$ in real space, and diagonalizing the resulting matrix using conjugate gradient algorithms[18]. The details of this calculation can be found in Ref. [31].

## III. MANY BODY SPECTRUM

To calculate the spectrum of interacting electrons, described by Hamiltonian $H$ in Eq.(1), we employ either the real space single particle or unrestricted Hartree-Fock states in configuration interaction techniques.[31] In the first SP-CI approach, single-particle levels are used to construct many-electron configurations which are the basis of configuration interaction (CI) Hamiltonian. Denoting the creation (annihilation) operators for electrons

in non-interacting SP state $|\alpha\sigma\rangle$ by $c_{\alpha\sigma}^{\dagger}$ ($c_{\alpha\sigma}$), the Hamiltonian of an interacting electron system in second quantization can be written as

$$\begin{aligned} H &= \sum_{\alpha} \sum_{\sigma} \epsilon_{\alpha} c_{\alpha\sigma}^{\dagger} c_{\alpha\sigma} \\ &+ \frac{1}{2} \sum_{\alpha\beta\gamma\mu} \sum_{\sigma\sigma'} V_{\alpha\sigma,\beta\sigma',\gamma\sigma',\mu\sigma} c_{\alpha\sigma}^{\dagger} c_{\beta\sigma'}^{\dagger} c_{\gamma\sigma'} c_{\mu\sigma} \end{aligned} \quad (3)$$

where the first term is the single particle Hamiltonian, and $V_{\alpha\sigma,\beta\sigma',\gamma\sigma',\mu\sigma} = \int d\vec{r} \int d\vec{r'} \varphi_{\alpha\sigma}^*(\vec{r}) \varphi_{\beta\sigma'}^*(\vec{r'}) \frac{e^2}{\epsilon|\vec{r}-\vec{r'}|} \varphi_{\gamma\sigma'}(\vec{r'}) \varphi_{\mu\sigma}(\vec{r})$, is the two-body Coulomb matrix element. In the configuration interaction method the Hamiltonian of an interacting system is calculated in the basis of finite number of many-electron configurations. The total number of configurations (or Slater determinants participating in CI calculation) is determined by

$$N_C = \left[ \frac{N_s!}{N_\uparrow! (N_s - N_\uparrow)!} \right] \left[ \frac{N_s!}{N_\downarrow! (N_s - N_\downarrow)!} \right]. \qquad (4)$$

Here $N_s$ is the number of single particle levels, and $N_\uparrow$ and $N_\downarrow$ are the number of spin up and spin down electrons. This Hamiltonian is either diagonalized exactly for small systems or low energy eigenvalues and eigenstates are extracted approximately for very large number of configurations.[31] With increasing the number of single-particle levels $N_s$, the number of configurations $N_C$ grows very fast, yet a large number is needed to accurately account for direct and exchange interaction, and electronic correlations. To improve the convergence of CI method we incorporate direct and exchange contribution into the basis states by replacing SP states with states obtained by the unrestricted Hartree-Fock method (URHF-CI). This implies expressing the new creation (annihilation) operators for URHF quasi-particles by $a_{i\sigma}^{\dagger}$ ($a_{i\sigma}$), with the index $i$ representing the URHF orbit quantum numbers. The URHF basis can be expanded in a linear combination of SP states. In terms of SP creation (annihilation) operators we write

$$a_{i\sigma}^{\dagger} = \sum_{\alpha=1}^{N_l} \lambda_{\alpha\sigma}^{(i)} c_{\alpha\sigma}^{\dagger}. \qquad (5)$$

The transformation coefficients, $\lambda_{\alpha\sigma}^{(i)}$, satisfy the self-consistent Pople-Nesbet equations[18,28,29,31]:

$$\begin{aligned} &\sum_{\gamma=1}^{N_l} \{ \epsilon_\mu \delta_{\gamma\mu} + \sum_{\alpha,\beta=1}^{N_l} (V_{\mu\alpha\beta\gamma} \sum_{\sigma'} \sum_{j=1}^{N_{\sigma'}} \lambda_{\alpha\sigma'}^{*(j)} \lambda_{\beta\sigma'}^{(j)} \\ &- V_{\mu\alpha\gamma\beta} \sum_{\sigma'} \sum_{j=1}^{N_{\sigma'}} \lambda_{\alpha\sigma'}^{*(j)} \lambda_{\beta\sigma'}^{(j)} \delta_{\sigma,\sigma'}) \} \lambda_{\gamma\sigma}^{(i)} = \epsilon_{i\sigma}^{HF} \lambda_{\mu\sigma}^{(i)}, \end{aligned} \quad (6)$$

where $\epsilon_{i\sigma}^{HF}$ are the URHF eigenenergies. The $N$-lowest energy URHF levels form a Slater determinant occupied

by HF quasi-electrons, corresponding to HF ground state. The rest of orbitals with higher energies are outside of the HF Slater determinant (unoccupied HF levels), contribute to electronic correlations, and can be used for CI calculation. The many body Hamiltonian of the interacting system in the URHF basis can finally be written as:

$$H = \sum_{\sigma}\sum_{ij}\langle i\sigma|T|j\sigma\rangle a_{i\sigma}^{\dagger}a_{j\sigma}$$
$$+\frac{1}{2}\sum_{ijkl}\sum_{\sigma}\sum_{\sigma'}U_{i\sigma,j\sigma',k\sigma',l\sigma}a_{i\sigma}^{\dagger}a_{j\sigma'}^{\dagger}a_{k\sigma'}a_{l\sigma}, \quad (7)$$

where $U_{i\sigma,j\sigma',k\sigma',l\sigma}$ are the Coulomb matrix elements in the URHF basis. Here

$$\langle i\sigma|T|j\sigma\rangle = \epsilon_{i\sigma}^{HF}\delta_{ij} - \langle i\sigma|U_H - U_X|j\sigma\rangle, \quad (8)$$

where $U_H$ and $U_X$ are the Hartree and exchange operators

$$\langle i\sigma|U_H|j\sigma\rangle = \sum_{\alpha\beta\mu\nu=1}^{N_l}V_{\alpha\mu\gamma\beta}\lambda_{\mu\sigma}^{*(i)}\lambda_{\gamma\sigma}^{(j)}\sum_{\sigma'}\sum_{k=1}^{N_{\sigma'}}\lambda_{\alpha\sigma'}^{*(k)}\lambda_{\beta\sigma'}^{(k)},$$

$$\langle i\sigma|U_X|j\sigma\rangle = \sum_{\alpha\beta\mu\nu=1}^{N_l}V_{\alpha\mu\beta\gamma}\lambda_{\alpha\sigma}^{*(i)}\lambda_{\beta\sigma}^{(j)}\sum_{k=1}^{N_{\sigma}}\lambda_{\mu\sigma}^{*(k)}\lambda_{\gamma\sigma}^{(k)}.$$

The resulting CI Hamiltonian matrix constructed in the basis of URHF configurations is either diagonalized exactly for small systems, or low energy eigenvalues and eigenstates are extracted approximately for very large number of configurations[31]. The details of the calculation and the convergence of the results as a function of number of basis and configurations, and comparison between SP-CI and URHF-CI methods can be found in Ref. 31.

## IV. SPIN TRANSITIONS IN A SINGLE DOT

We describe a single dot by an isotropic gaussian confining potential $V(x,y) = V_0 e^{-(x^2+y^2)/\Delta^2}$. The single particle eigenenergies of such quantum dot as a function of cyclotron frequency $\omega_c = eB/m^*$ are shown in Fig. 1.

States with spin up (down) are shown by bold (dashed) lines. For illustration, a very large g-factor is introduced. We note in Fig. 1, with increasing magnetic field the energy of spin up (bold) levels decrease. These levels, and their spin down partners, correspond to the levels of the lowest Landau level (LLL). We now populate the lowest energy states with a number of electrons. From previous work[5], the minimum number of electrons which exhibits all nontrivial phenomena in the spin evolution of a single quantum dot is $N = 4$. The $N = 4$ configurations which minimize the kinetic and Zeeman energy are shown in Fig.1. Due to the crossing of spin up and down levels,
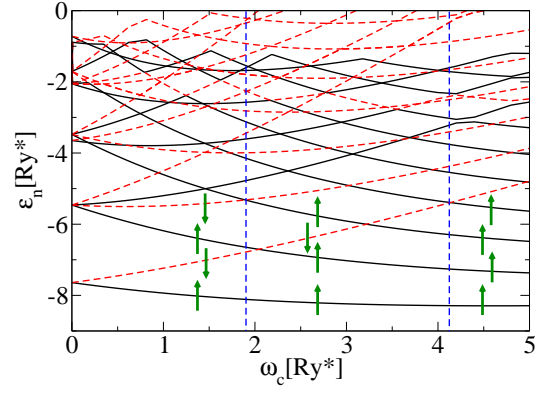


FIG. 1: (Color online) Single particle spectrum as a function of cyclotron frequency $\omega_c$ for a gaussian single dot with strength $V_0 = -10Ry^*$, and $\Delta = 2.5a_0^*$ in the presence of Zeeman splitting. Arrows represent spin of electrons. For illustration purposes a very high Zeeman coupling $g = -9$ is used.
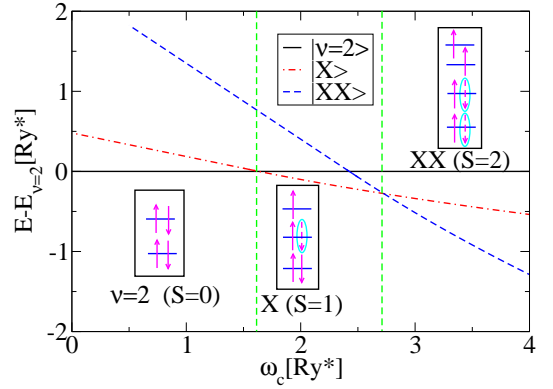


FIG. 2: (Color online) The energy of spin configurations shown in the boxes, $|\nu = 2\rangle$, $|X\rangle$, and $|XX\rangle$ with total spin $S = 0$, $S = 1$, and $S = 2$, using LLL orbitals, and $E_Z = 0$. $E_{\nu=2}$ $(S = 0)$ is the reference of energy. The arrows surrounded by circles represent the holes.

there are three different configurations $S_z = 0$, $S_z = 1$, and $S_z = 2$. These configurations illustrate increasing spin polarization of the electronic droplet with increasing magnetic field. With very small Zeeman energy the increasing spin polarization in quantum dots is driven by electron-electron interactions. We hence turn off the Zeeman coupling and turn on electron-electron interactions.

We start with the lowest energy configuration build with SP LLL states, the $S_z = 0$ spin singlet $\nu = 2$ configuration $|\nu = 2\rangle$. The spin excitations with $S = 1$ and $S = 2$, are constructed by removing electrons from occupied states and putting to unoccupied states, and can be described in terms of single exciton $|X\rangle$ and biexciton $|XX\rangle$ configurations, as shown in Fig. 2. Neglecting the mixing between configurations, we calculate the energy of each spin configuration. The result of this calculation is
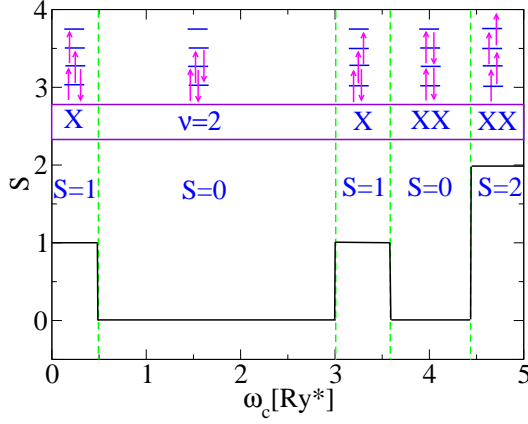
FIG. 3: (Color online) The spin evolution of the ground state of single quantum dot as a function of magnetic field using URHF-CI method with $N_s = 8$ HF levels, corresponding to $N_C = 784$ configurations.

shown in Fig. 2. We chose the energy of the $S = 0, \nu = 2$ state ($E_{\nu=2}$) as the reference energy. As shown in Fig. 2, with increasing magnetic field even without Zeeman energy both the first and second spin flip transitions occur at $\omega_c = 1.6$ and $\omega_c = 2.75$ due to electron-electron interactions.

The effect of correlations on the evolution of spin of electrons in a single quantum dot obtained by the URHF-CI method is shown in Fig. 3. Here the spin unpolarized ($S_z = 0$) URHF states have been constructed out of $N_l = 30$ SP states. $N_s = 8$ HF levels have be taken to construct CI Hamiltonian, resulting in $N_C = 784$ configurations. At zero magnetic field we find $S = 1$ triplet due to Hund's rule for electrons in a half-filled p-shell. With increasing magnetic field, the single particle energy gap opens up, leading to suppression of the $S = 1$ triplet state, and formation of the $\nu = 2$ ($S = 0$) singlet state. The first spin flip $S = 1$ state appears around $\omega_c = 3$, followed by the second spin flip spin polarized $S = 2$ state at $\omega_c = 4.5$. The flipping of the second spin is interrupted by a low-spin, $S = 0$, strongly correlated state. This state was previously identified with the formation of spin singlet bi-exciton.[5] The first and second spin flip state can be obtained both for the noninteracting electrons and in Hartree-Fock approximation while the formation of spin singlet bi-exciton is a result of electronic correlations in a quantum dot.

## V. SPIN TRANSITIONS IN QUANTUM DOT MOLECULES

We now turn to study the spin transitions of laterally coupled quantum dots. We describe the molecule by electron ($N_L, N_R$) and ground state spin numbers ($S_L, S_R$) of isolated left (L) and right (R) dots. The spin phase diagram turns out to depend on electron numbers in each dot. Here we will focus on molecules build out of identical

dots with $N_L = N_R$. For a given number of electrons the magnetic field will be used to tune their individual spin $S_L = S_R$. The goal will be to determine the total spin of the molecular system. The molecular coupling will be controlled by the height of the tunneling barrier. To illustrate the physics we will discuss in detail quantum dot molecule $(4, 4)$ with four electrons each and contrast its properties with a single $N = 4$ quantum dot discussed in previous section.

## A. One electron spectrum of a quantum dot molecule

We parameterize quantum dot molecule potential in terms of a sum of three Gaussians $V(x, y) = V_L \exp[-\frac{(x+a)^2+y^2}{\Delta^2}] + V_R \exp[-\frac{(x-a)^2+y^2}{\Delta^2}] + V_p \exp[-\frac{x^2}{\Delta_{Px}^2} - \frac{y^2}{\Delta_{Py}^2}]$. Here $V_L, V_R$ describe the depth of the left and right quantum dot minima located at $x = -a, y = 0$ and $x = +a, y = 0$, and $V_p$ is the central plunger gate potential controlling the tunneling barrier. The confining potential is parameterized as $V_L = V_R = -10, \Delta = 2.5, a = 2$, and $\Delta_{Px} = 0.3$, $\Delta_{Py} = 2.5$, in effective atomic units. The single particle eigenvalues and eigenfunctions are calculated numerically by discretization of the Schrödinger equation with the quantum dot molecule potential. The parameters of the confining potential considered in this work are chosen to represent weakly coupled quantum dots. At zero magnetic field the SP levels of the electrons exhibit well separated S,P, and D electronic shells, and at high magnetic field they form molecular shells of closely spaced pairs of bonding-antibonding orbitals. The half-filled molecular shells correspond to electron numbers ($N_L = 2k - 1, N_R = 2k - 1$) and filled shells correspond to ($N_L = 2k, N_R = 2k$) configurations ($k$ is integer). The resulting single particle spectrum as a function of magnetic field has been presented recently in Fig. 1 of Ref. 21. In order to understand and visualize the spectrum in high magnetic field we expand confining potential in the vicinity of each minimum. This gives a parabolic potential $V(r) = m^*\omega_0^2 r^2/2$ with the strength $\omega_0 = 2\sqrt{|V_0|/\Delta^2}$. The low energy spectrum of each dot corresponds to two harmonic oscillators with eigen-energies $\epsilon_{nm} = \omega_+(n + 1/2) + \omega_-(m + 1/2)$. Here $\omega_\pm = \sqrt{\omega_0^2 + \omega_c^2/4} \pm \omega_c/2$, $\omega_c$ is the cyclotron energy, and $n, m = 0, 1, 2, ....$ With increasing magnetic field the $\omega_-$ decreases to zero while $\omega_+$ approaches the cyclotron energy $\omega_c$, and the states $|m, n\rangle$ evolve into the nth Landau level. In high magnetic field the corresponding wavefunctions admit a description in terms of localized LLL orbitals[18]. In this limit linear combinations of the LLL orbitals $m$ from left and right dot forms molecular shells of closely spaced symmetric-antisymmetric pairs with eigen-energies expressed approximately as

$$\epsilon_{m\lambda\sigma} = \omega_-(m + \frac{1}{2}) - \lambda\frac{\Delta_m}{2} - \frac{1}{2}\sigma\gamma\omega_c. \qquad (9)$$

Here $E_Z = \gamma\omega_c$ is the Zeeman energy, $\sigma = +1$ ($-1$) corresponds to spin $\uparrow$ ($\downarrow$), $\gamma = m^*g$ and $\lambda$ is the pseudospin index: the symmetric (antisymmetric) orbitals are labeled by $\lambda = +1$ ($-1$), the parity of the molecular orbitals. $\Delta_m$ is the symmetric-antisymmetric gap. The Zeeman coupling induces spin splitting with increasing magnetic field. This has been illustrated in Fig. 1 of Ref. 21. We now populate the quantum dot molecule with $N = 8$ electrons. This is an example of electronic configurations corresponding to filled molecular shells. Fig. 1 of Ref. 21 shows the evolution of the lowest energy states of noninteracting electrons, with the corresponding total spin $S$ states separated by vertical lines. We find $S = 0, 2$, and 4 phases with even $S$ which correspond to simultaneous spin flips in each isolated dot.

However, we also find odd $S$ phases. The first odd spin state with $S = 1$ occurs between magnetic fields corresponding to $\omega_{c1}^* \approx 3.25$ and $\omega_{c2}^* \approx 3.9$ where $\epsilon_{m=2,\sigma=\uparrow,\lambda=+1} = \epsilon_{m=1,\sigma=\downarrow,\lambda=-1}$, and $\epsilon_{m=2,\sigma=\uparrow,\lambda=-1} = \epsilon_{m=1,\sigma=\downarrow,\lambda=+1}$. The odd spin flip is related to the splitting of energy levels due to tunneling. Using single particle eigen-energies given by Eq.(9), we find the first spin flip at the value of the magnetic field $B_1$

$$\gamma\omega_c(1) = \omega_-(1) - \frac{\Delta_2(1) + \Delta_1(1)}{2} \qquad (10)$$

where Zeeman energy equals the single dot level splitting minus the average symmetric-antisymmetric gap for the two levels involved. The second spin flip takes place at $\omega_c(2)$ such that

$$\gamma\omega_c(2) = \omega_-(2) + \frac{\Delta_2(2) + \Delta_1(2)}{2}. \qquad (11)$$

Hence the difference in the magnetic fields corresponding to first and second spin flips is a direct measure of the tunneling splitting:

$$\gamma(\omega_c(2) - \omega_c(1)) = \frac{\Delta_2(2) + \Delta_1(2)}{2} + \frac{\Delta_2(1) + \Delta_1(1)}{2}. \qquad (12)$$

From the spectrum of Fig. 1 of Ref. 21, we observe that the states with odd spins $S = 1$, and $S = 3$, are stable within narrow range of magnetic fields due to spin flip transitions among the electrons that occupy the levels with energy separation proportional to the inter-dot tunneling amplitude. This is in contrast with the first spin flip transition in single dots (compare with Fig. 1) which is stable in a wide range of magnetic fields. For this reason the existence of odd spin states in the spin phase diagram of quantum dot molecules can be interpreted as the measure of inter-dot interaction.

## B. Many electron quantum dot molecule spectrum

In this section we present an analysis of spin transitions driven by electron-electron interaction. We focus on the tunnel coupled lowest Landau level orbitals $m$. Denoting the creation (annihilation) operators for electron in non-interacting SP state $|m\lambda\sigma\rangle$ by $c_{m\lambda\sigma}^\dagger$ ($c_{m\lambda\sigma}$) (with $\sigma$ as spin label), the Hamiltonian of an interacting system, Eq. 1, can be written as

$$
\begin{aligned}
H = & \sum_{m\lambda}\sum_\sigma \epsilon_{m\lambda\sigma}c_{m\lambda\sigma}^\dagger c_{m\lambda\sigma} \\
& + \frac{1}{2}\sum_{\{m,\lambda\}}\sum_{\sigma\sigma'}\langle m_1\lambda_1\sigma, m_2\lambda_2\sigma'|V|m_3\lambda_3\sigma', m_4\lambda_4\sigma\rangle \\
& \times c_{m_1\lambda_1\sigma}^\dagger c_{m_2\lambda_2\sigma'}^\dagger c_{m_3\lambda_3\sigma'}c_{m_4\lambda_4\sigma}
\end{aligned} \qquad (13)
$$

The single particle states of coupled quantum dot molecules in magnetic field are labeled by the orbital quantum numbers $m$, and the pseudospin index $\lambda$. The first term in Eq. 13 is the single particle Hamiltonian, and $V_{\alpha\beta\mu\nu}$ is the two-body Coulomb matrix element. Here $\{\alpha, \beta, \mu, \nu\}$ represent the states with quantum numbers $(m, \lambda, \sigma)$. We now turn to the construction of the relevant configurations.

### C. $S = 0$, $\nu = 2$ state

The $\nu = 2$ state of quantum dot molecule with $N$ electrons and total spin $S = 0$, shown in Fig. 4, is the product of electron creation operators

$$|\nu = 2\rangle = \prod_{m=0}^{N/4-1}\prod_{\lambda=1,2}\prod_{\sigma=\uparrow,\downarrow}c_{m\lambda\sigma}^\dagger|0\rangle \qquad (14)$$

The energy associated with this state

$$E_{\nu=2} = \sum_{m=0}^{N/4-1}\sum_{\lambda=\pm 1}\sum_\sigma[\epsilon_{m\lambda\sigma} + \Sigma(m, \lambda, \sigma)] \qquad (15)$$

can be expressed in terms of self-energy $\Sigma(m, \lambda, \sigma)$

$$
\begin{aligned}
\Sigma(m, \lambda, \sigma) = & \sum_{m'=0}^{N/4-1}\sum_{\lambda'=\pm 1}(2\langle m\lambda, m'\lambda'|V|m'\lambda', m\lambda\rangle \\
& - \langle m\lambda, m'\lambda'|V|m\lambda, m'\lambda'\rangle).
\end{aligned} \qquad (16)
$$

### D. $S = 1$ spin exciton

The $S = 1$ spin flip excitation is constructed by removing an electron from occupied $j$ orbital in a $\nu = 2$ state, and putting it into an unoccupied state $i$,

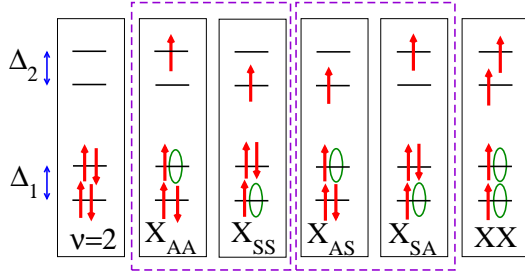$$|X_{j\rightarrow i}\rangle = c_i^\dagger c_j|\nu = 2\rangle, \qquad (17)$$

FIG. 4: (Color online) The basis of spin configurations in high magnetic fields. The first spin transition states $S = 1$ identify with two independent set: $\{X_{SS}, X_{AA}\}$, and $\{X_{SA}, X_{AS}\}$. In the former the electron-hole transitions occurs between the states with the same symmetry and hence they do not mix with the latter which exhibit the process of electron-hole excitations between states with opposite parity.



FIG. 5: (Color online) The lowest energy excitons in real space $|X_{RR}\rangle = |X_{(1,R,\downarrow)\to(2,R,\uparrow)}\rangle$, $|X_{LL}\rangle = |X_{(1,L,\downarrow)\to(2,L,\uparrow)}\rangle$, $|X_{RL}\rangle = |X_{(1,R,\downarrow)\to(2,L,\uparrow)}\rangle$, and $|X_{LR}\rangle = |X_{(1,L,\downarrow)\to(2,R,\uparrow)}\rangle$. The magnetic ordering of these states can be described by means of ferrimagnetic coupling $(S_L = 0, S_R = 1)$ for $X_{RR}$, and $(S_L = 1, S_R = 0)$ for $X_{LL}$, and ferromagnetic coupling $(S_L = 1/2, S_R = 1/2)$ for $X_{RL}$, and $X_{LR}$.

where $j \equiv (m, \lambda, \downarrow)$, and $i \equiv (m', \lambda', \uparrow)$. Denoting quasi-particle energy levels (electrons dressed by interaction) by $\varepsilon_i = \epsilon_i + \Sigma(i)$ the energy of one exciton follows

$$\Delta E_{X_{j\to i}} = \varepsilon_i - \varepsilon_j - \langle i, j|V|j, i\rangle \qquad (18)$$

where $\Delta E_{X_{j\to i}} = E_{X_{j\to i}} - E_{\nu=2}$ is the energy of exciton relative to the $\nu = 2$ state energy. The last term in Eq. (18) is the electron-hole Coulomb attraction. The lowest energy states of the single exciton corresponding to the first spin flip state are depicted in Fig. 4. We classify the single excitons based on their relative parity with respect to the parity of the $\nu = 2$ state. Pair of states $(X_{SS}, X_{AA})$ describes transitions between pairs of levels with the same parity and so parity is conserved by these transitions. In contrast, spin flip transitions represented by $(X_{SA}, X_{AS})$ do not conserve parity as they describe transitions between pairs of levels with opposite parity. We identify $(X_{SS}, X_{AA})$, and $(X_{SA}, X_{AS})$ by their parity quantum numbers $\pi = +1$ and $\pi = -1$, respectively. It is important to note that Coulomb interactions do not mix excitons with different parities, and the CI Hamiltonian constructed in the basis of spin excitons is block diagonal. These pairs of independent excitons are shown inside the boxes in Fig. 4.

In real space, single excitons can be expressed in terms of linear combination of excitons localized in each dot. This basis is shown in Fig. 5. In each isolated dot, at a critical field, a transition from the $S = 0$ singlet to the $S = 1$ triplet state takes place. This configuration, corresponding to $X_{RR}$ and $X_{LL}$ in Fig. 5, is equivalent to a localized electron-hole excitation in one dot in the presence of background of electrons in the other dot. Because of the geometrical symmetry associated with the electron-hole excitation, the ground state of the system without external bias and interdot tunneling has double degeneracy: The state with $(S_L = 0, S_R = 1)$ has exactly the same energy as the state $(S_L = 1, S_R = 0)$. The many body wavefunction of such a molecular state can

be expressed as linear combination of degenerate states $|S_L = 0, S_R = 1\rangle$ and $|S_L = 1, S_R = 0\rangle$. We identify these pairs of molecular states with quantum Hall ferrimagnets. For a range of magnetic field these two states are separated from another pair of single excitations $X_{LR}$ and $X_{RL}$ with $(S_L = 1/2, S_R = 1/2)$ by an energy gap due to Coulomb interactions. In general, in the case of filled shells, molecular states with odd total spin $S$ correspond to quantum Hall ferrimagnets. Our analysis of spin transitions in real space is presented in section VI.

### E. $S = 2$ spin bi-exciton

With increasing magnetic fields, a higher polarized state with $S = 2$, $(S_L = 1, S_R = 1)$ equivalent to a spin bi-exciton state appears. A bi-exciton is constructed by removing a pair of electrons from occupied states and putting them into unoccupied states (see Fig. 4),

$$|XX_{j\to i, k\to l}\rangle = c_i^\dagger c_l^\dagger c_j c_k |\nu = 2\rangle. \qquad (19)$$

The energy of biexciton can be decomposed into the energy of two single excitons plus their interaction

$$\Delta E_{XX_{j\to i, k\to l}} = \Delta E_{X_{j\to i}} + \Delta E_{X_{k\to l}} + \delta V, \qquad (20)$$

where $\Delta E_{X_{j\to i}}$ has been defined in Eq. 18. $\delta V$ is the binding energy between two excitons, accounting for the electron-electron, electron-hole and hole-hole interactions

$$\begin{aligned}
\delta V &= \langle l, i|V|i, l\rangle - \langle l, i|V|l, i\rangle \\
&\quad - \langle l, j|V|j, l\rangle - \langle k, i|V|i, k\rangle \\
&\quad + \langle j, k|V|k, j\rangle - \langle j, k|V|j, k\rangle. \qquad (21)
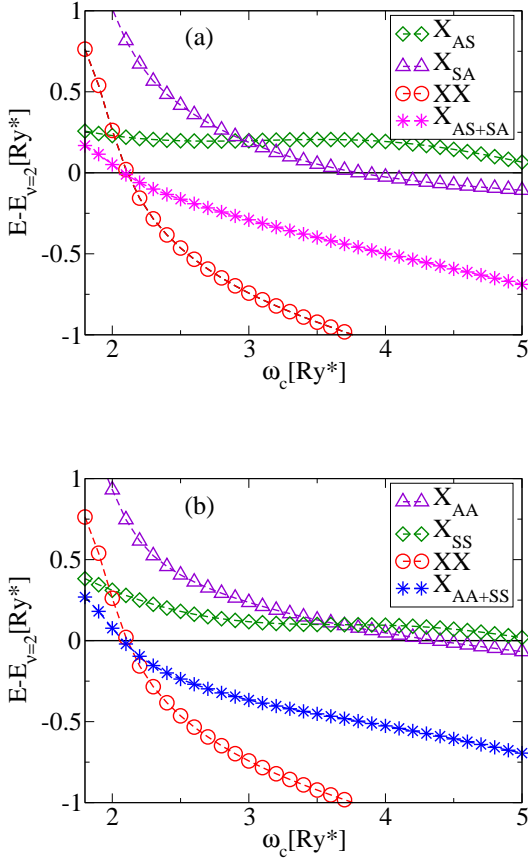\end{aligned}$$

FIG. 6: (Color online) (a) The energies of two single spin excitons $X_{SA}$ and $X_{AS}$ with odd parity, the energy of the odd parity correlated exciton $X_{SA+AS}$, and the energy of the spin bi-exciton $S = 2$ state as a function of magnetic field. All energies measured from the energy of the $\nu = 2, S = 0$ state. (b) The energies of two single spin excitons $X_{SS}$ and $X_{AA}$ with even parity, the energy of the even parity correlated exciton $X_{SS+AA}$, and the energy of the spin bi-exciton $S = 2$ state as a function of magnetic field. All energies measured from the energy of the $\nu = 2, S = 0$ state.

## F.  First versus second spin flip in a quantum dot molecule

Unlike in a single quantum dot, first spin flip state $S = 1$ is not an eigenstate of the coupled quantum dot Hamiltonian. There are two possible spin excitons for a given parity, and they are coupled by Coulomb interactions. We use two distinct single exciton basis $\{X_{SS}, X_{AA}\}$ and $\{X_{SA}, X_{AS}\}$, labeled by parity $\pi = +1$ and $\pi = -1$, to construct the two $2\times 2$ Hamiltonians. We denote by $\Delta E_{X_{SS+AA}}$, $\Delta E_{X_{SA+AS}}$ the lowest eigen-energies of these Hamiltonians.

Fig. 6(a) shows the numerically calculated energies of odd parity spin excitons as a function of magnetic field.

The energy $\Delta E_{X_{AS}}$ of spin exciton $X_{AS}$ is positive for magnetic fields shown but the energy $\Delta E_{X_{SA}}$ of spin exciton $X_{SA}$ becomes negative at $\omega_c = 3.8$ i.e. the $X_{SA}$ spin flip state becomes the lower energy state than the $\nu = 2, S = 0$ state. However, in stark contrast with a single quantum dot, Fig. 2, we find that the second spin flip state $XX$ becomes the ground state at lower magnetic field $\omega_c = 2.1$. Hence, unlike in a single quantum dot we find a transition from spin singlet $S = 0$ state directly to $S = 2$ second spin flip state. This is a transition corresponding to even total spin numbers, as if the two dots were flipping their spin simultaneously. However, correlations or mixing of the two spin excitons $X_{AS}$ and $X_{SA}$ lowers the energy of the spin exciton. The energy $\Delta E_{X_{SA+AS}}$) of the correlated single spin state is significantly lower and equals both the energy $\Delta E_{XX}$ of the second spin flip bi-exciton and of the $\nu = 2, S = 0$ state at $\omega_c = 2.1$. At this value of the magnetic field the energy of the bi-exciton and of the exciton are almost identical, and we might expect that for larger number of configurations correlations will stabilize the single spin flip exciton even further. The effect of correlations on the even parity excitons $X_{AA}$ and $X_{SS}$ is shown in Fig. 6(b). We see that mixing of the two even parity excitons lowers the energy $\Delta E_{X_{SS+AA}}$ of the correlated single spin state. This energy equals both the energy $\Delta E_{XX}$ of the second spin flip bi-exciton and of the $\nu = 2, S = 0$ state at $\omega_c = 2.1$. By comparison with Fig. 6(a) we see that the value of $\omega_c = 2.1$ also corresponds to the change in parity of the single spin exciton $S = 1$ state.

As illustrated in Fig. 6, with mixing of single exciton configurations the energy of quantum dot molecule exhibits four-fold degeneracy at $\omega_{c1}^*$ where $S = 0$, $S = 2$ and two different parity $S = 1$ states become the lowest energy states. The $S = 1$ states show stability in a narrow range of magnetic field, within the accuracy of our numerical results. With further increase of magnetic field, single excitons condense into pairs of excitons forming bi-excitons. The existence of single, odd, spin excitons is hence a signature of electronic correlations. These states do not exist at the Hartree-Fock level.

To support the assertion that correlations are responsible for the existence of odd spin excitons we employ URHF-CI calculation. From the solution of the Pople-Nesbet equations we obtain HF eigen-energies, shown in Fig. 7 (a), for $N = 8$ electrons with $S_z = 0$, as a function of the magnetic field. The HF wavefunctions are used as a basis in HF-CI calculation of the ground state. We employ $N_s = 8$ HF basis states (equivalent to $N_C = 4900$ configurations) to calculate the total spin of electrons in quantum dot molecule as a function of the magnetic field. From this calculation we find that the $S = 0$, $S = 1$, and $S = 2$ states are almost degenerate at $\omega_{c1}^* = 3.1$. The prediction of URHF-CI is in qualitative agreement with effective SP-CI model, presented above. The direct, exchange, and correlation energies calculated by URHF-CI shift the transition point to higher magnetic fields.

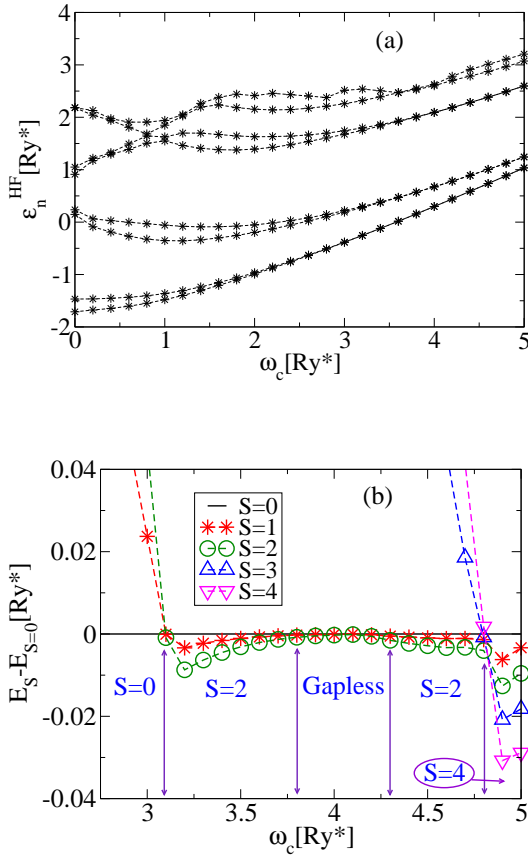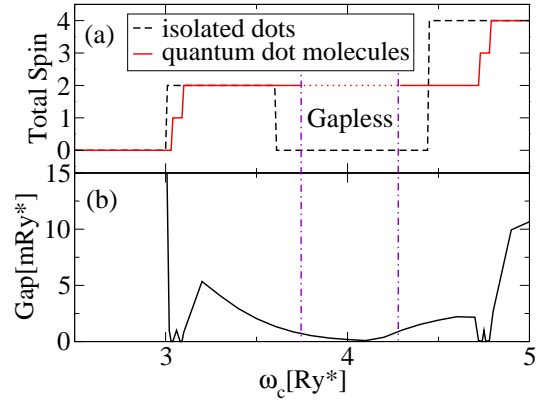With increasing of the magnetic field we find that the

FIG. 8: (Color online) (a) The evolution of spin of the $N = 8$ electron quantum dot molecules as a function of magnetic field for $g = 0$ and $V_p = 7$ (solid line). For comparison the spin evolution of two isolated dots is shown (dashed line). The width of odd spin plateaux have been artificially enlarged to be visible by eyes. The vertical dashed line (with purple-color online) tends to show qualitatively a range of $\omega_c$ in which the gap vanishes. The horizontal dashed line (with red-color online) shows the corresponding spin one state with zero gap. (b) The evolution of the energy gap of the quantum dot molecules as a function of magnetic field.



FIG. 7: (Color online) (a) URHF energies vs. cyclotron energy for $N = 8$ electrons with $S_z = 0$. (b) Evolution of lowest energies for $S = 0, 1, 2$ states calculated by URHF-CI method. The energies are measured from the energy of the $S = 0$ state.
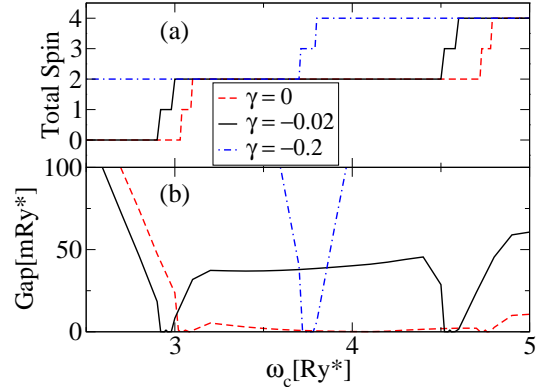


FIG. 9: (Color online) The effect of increasing Zeeman energy on the (a) evolution of spin and (b) evolution of energy gap of the $N = 8$ electron quantum dot molecules as a function of magnetic field. The width of $g = 0$ odd spin plateaux have been artificially enlarged to be visible by eyes.

gap between different total spin states tends to vanish. This gapless phase is seen in Figs. (7) and (8) in the vicinity of $\omega_c = 4$. This phase is followed by the $S = 2$, $S = 3$ and $S = 4$ states. The latter state corresponds to a fully spin polarized $\nu = 1$ droplet.

Let us now summarize the similarities and the differences in the evolution of total spin of two isolated dots and a quantum dot molecule. Fig. 8 (a) shows the evolution of total spin with increasing magnetic field for two noninteracting $N = 4$ quantum dots and for $N = 8$ quantum dot molecule. Fig.8(b) shows the energy gap of the molecule as a function of magnetic field. The noninteracting quantum dots spin evolution is obtained by adding results from two isolated dots, each dot evolving with magnetic field according to Fig. 3. We find that the effect of interdot interaction is to renormalize the magnetic fields at which spin transitions take place, and more importantly, to lead to the appearance of odd spin states $S = 1$ and $S = 3$. While the existence of odd spin states is most striking, the presence of spin polarized phases is also nontrivial. The fact that spins of electrons on two quantum dots align demonstrates the existence of ferromagnetic dot-dot coupling. In the case of antifer-

romagnetic coupling there would have been no net spin eventhough each dot has finite spin. We will show in the next section that such antiferromagnetic coupling exists in the $N = 8$ molecule at low magnetic fields.

Finally, following the gap in Fig.8(b) we find the existence of low spin "gapless" states, molecular analogs
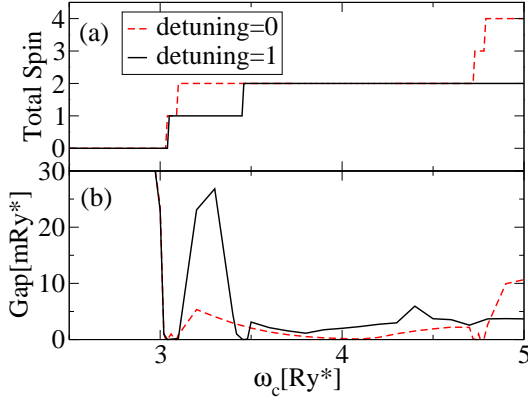
FIG. 10: (Color online) The effect of detuning, i.e., difference in confining potential between left dot $V_L$ and right dot $V_R$ on the (a) evolution of spin and (b) evolution of energy gap of the $N = 8$ electron quantum dot molecules as a function of magnetic field.

of spin singlet bi-excitons. Hence Fig.8 shows that electronic inter-dot correlations stabilize the odd spin phases but their stability range is very narrow. As shown in Sec. (V A) without electron-electron interactions competition between quantum mechanical tunneling and Zeeman energy was responsible for the existence of odd spin phases. The effect of finite Zeeman energy is similar in an interacting system. Fig.9 shows the effect of increasing Zeeman energy on the evolution of spin and energy gap of the $N = 8$ electron quantum dot molecules as a function of magnetic field. All parameters are the same as in Fig.8. We see that increasing Zeeman energy renormalizes the magnetic field value of spin flips and, more importantly, stabilizes the odd spin phases. From the evolution of the energy gap shown in Fig.9b we also see the vanishing of the low spin depolarized phase in the vicinity of $\omega_c = 4$ and the stabilization of the spin polarized $S = 2$ phase. The Zeeman energy depends on the g-factor. For GaAs the g-factor is $g_{GaAs} = -0.44$ while for InAs and InSb the g-factors are $g_{InAs} = -14$, and $g_{InSb} = -50$.[8,9,10,11,32,33] Hence by adding In one can hope to tune the g-factor of quantum dot molecules.

To conclude our analysis of the $N = 8$ electron quantum dot molecule we discuss the effect of asymmetry between the two dots. While for molecules built out of two atoms each component is identical, quantum dots are defined by gates or etching and one must understand the effect of differences between the two dots on the stability diagram[30]. In Fig.10 we show the evolution of spin and energy gap of the $N = 8$ electron quantum dot molecules as a function of magnetic field. The two dots are different, with confining potential of the left dot $V_L = -10$ unchanged but the potential of the right dot detuned by $1Ry$ to $V_R = -11$. As anticipated, the effect of detun-

ing results in increased stability of the odd spin flip state $S = 1$.

## VI. REAL SPACE ANALYSIS OF SPIN TRANSITIONS IN QUANTUM DOT MOLECULES

In this section, we describe the analysis of spin transitions in real space. Eq. (13) describes the Hamiltonian of an interacting system in second quantization in non-interacting SP state $|m\lambda\sigma\rangle$. The single particle states of coupled quantum dot molecules in magnetic field are labeled by the single dot orbital quantum numbers $m$, and the pseudospin index $\lambda$. The symmetric (antisymmetric) orbitals are labeled by $\lambda = 1$ $(-1)$, the parity of the orbitals in two symmetric dots. $m$ represents the combined Landau level, and angular momentum quantum numbers, $m \equiv (n, l)$. The first term in Eq. (13) is the single particle Hamiltonian, and $V_{\alpha\sigma,\beta\sigma',\mu\sigma',\nu\sigma} = \int d\vec{r} \int d\vec{r'} \tilde{\varphi}^*_{\alpha\sigma}(\vec{r}) \tilde{\varphi}^*_{\beta\sigma'}(\vec{r'}) \frac{e^2}{\epsilon|\vec{r}-\vec{r'}|} \tilde{\varphi}_{\mu\sigma'}(\vec{r'}) \tilde{\varphi}_{\nu\sigma}(\vec{r})$, is the two-body Coulomb matrix element. Here $\{\alpha, \beta, \mu, \nu\}$ represent the states with orbital quantum numbers $(m, \lambda)$.

Alternatively denoting the creation (annihilation) operators for electron in non-interacting localized SP state $|ms\sigma\rangle$ by $d^\dagger_{ms\sigma}$ ($d_{ms\sigma}$), the Hamiltonian of an interacting system in second quantization can be written as

$$
\begin{aligned}
H &= \sum_{ms} \sum_\sigma \tilde{\epsilon}_{ms} d^\dagger_{ms\sigma} d_{ms\sigma} \\
&+ \sum_{m\sigma} t_m \sum_{s_1 s_2} (1 - \delta_{s_1 s_2}) d^\dagger_{ms_1\sigma} d_{ms_2\sigma} \\
&+ \frac{1}{2} \sum_{\{m,s\}} \sum_{\sigma\sigma'} \langle m_1 s_1 \sigma, m_2 s_2 \sigma' | V | m_3 s_3 \sigma', m_4 s_4 \sigma \rangle \\
&\times d^\dagger_{m_1 s_1 \sigma} d^\dagger_{m_2 s_2 \sigma'} d_{m_3 s_3 \sigma'} d_{m_4 s_4 \sigma}
\end{aligned}
\tag{22}
$$

Here $s = 1$ (2) are pseudospin labels of electron localized in left (right) dot. The relation between Eqs. 13, and 22 can be established by a rotation in pseudospin space $c^\dagger_{m\lambda\sigma} = \frac{1}{\sqrt{2}} \sum_{s=1}^2 \lambda^{s-1} d^\dagger_{ms\sigma}$. We find $\tilde{\epsilon}_{ms} = (\epsilon_{m,\lambda=1} + \epsilon_{m,\lambda=-1})/2$, $t_m = (\epsilon_{m,\lambda=1} - \epsilon_{m,\lambda=-1})/2$, and

$$
\langle m_1 s_1 \sigma, m_2 s_2 \sigma' | V | m_3 s_3 \sigma', m_4 s_4 \sigma \rangle = \frac{1}{4} \sum_\lambda \lambda_1^{s_1-1} \lambda_2^{s_2-1}
$$

$$
\lambda_3^{s_3-1} \lambda_4^{s_4-1} \langle m_1 \lambda_1 \sigma, m_2 \lambda_2 \sigma' | V | m_3 \lambda_3 \sigma', m_4 \lambda_4 \sigma \rangle \tag{23}
$$

### A. $S = 0$ ground state

The $\nu = 2$ state of quantum dot molecule with $N$ electrons and total spin $S = 0$ is the product of spin polarized localized electrons

$$
|\nu = 2\rangle = \prod_{m=0}^{N/4-1} \prod_{s=1,2} \prod_{\sigma=\uparrow,\downarrow} d^\dagger_{ms\sigma} |0\rangle \tag{24}
$$

The energy associated with this state follows

$$E_{\nu=2} = \sum_{m=0}^{N/4-1} \sum_{s=1}^{2} (2\tilde{\epsilon}_{ms} + \Sigma(m,s)) \qquad (25)$$

where $\Sigma(m,s)$ is the electron self-energy:

$$\begin{aligned}
\Sigma(m,s) &= \sum_{m'=0}^{N/4-1} \sum_{s'=1}^{2} (2\langle ms, m's'|V|m's', ms\rangle \\
&\quad - \langle ms, m's'|V|ms, m's'\rangle) \qquad (26)
\end{aligned}$$

### B. $S = 1$ exciton

In each isolated dot, at a critical field, and driven by electron-electron Coulomb interaction and increasing electron kinetic energy, a transition from $S = 0$ singlet to $S = 1$ triplet is seen. The cost in kinetic energy is lowered if localized electrons in one dot flip the spin ($S_L = 1$), while the other electrons in the second dot occupy the lowest energy single particle states to form spin singlet droplet ($S_R = 0$). This configuration corresponding to $X_{RR}$ (or $X_{LL}$) in Fig. 5, is equivalent to a localized electron-hole excitation in one dot in the presence of the background of electrons in the other dot. Because of the geometrical symmetry associated with the electron-hole excitation, the ground state of the system (without any external bias and interdot tunneling) has double degeneracy: The state with ($S_L = 0, S_R = 1$) has exactly the same energy as the state ($S_L = 1, S_R = 0$). The many body wavefunction of such a molecular state can be expressed as linear combination of degenerate states $|S_L = 0, S_R = 1\rangle$, and $|S_L = 1, S_R = 0\rangle$. We identify these pairs of excitations as quantum Hall ferrimagnets. For a range of magnetic fields these two states are separated from another pair of single excitations $X_{LR}$ and $X_{RL}$ with ($S_L = 1/2, S_R = 1/2$) by an energy gap due to Coulomb interaction.

An excitonic state is constructed by removing an electron from occupied state and putting into an unoccupied state

$$|X_{j\to i}\rangle = d_i^\dagger d_j |\nu = 2\rangle \qquad (27)$$

where $j \equiv (m, s, \downarrow)$, and $i \equiv (m', s', \uparrow)$ The lowest energy basis of the single exciton (first spin flip state) is depicted in Fig. 5. Labeling the direct and indirect spin flip transitions (with ferrimagnetic and ferromagnetic spin ordering) by $\{X_{RR}, X_{LL}\}$, and $\{X_{LR}, X_{RL}\}$ and using their symmetries we find that the direct (indirect) states are two-fold degenerate $E_{X_{RR}} = E_{X_{LL}}$ ($E_{X_{LR}} = E_{X_{RL}}$). Here the subscripts are defined as $RR \equiv (1, R, \downarrow) \to (2, R, \uparrow)$, $LL \equiv (1, L, \downarrow) \to (2, L, \uparrow)$, $RL \equiv (1, R, \downarrow) \to (2, L, \uparrow)$, and $LR \equiv (1, L, \downarrow) \to (2, R, \uparrow)$. Note that in non-interacting system the basis is four fold degenerate $E_{X_{RR}} = E_{X_{LL}} = E_{X_{LR}} = E_{X_{RL}}$.

Denoting quasi-particle energy levels by $\varepsilon_i = \tilde{\epsilon}_i + \Sigma(i)$, the energy of one exciton reads

$$E_{X_{j\to i}} = E_{\nu=2} + \varepsilon_i - \varepsilon_j - \langle i, j|V|j, i\rangle, \qquad (28)$$

where the last term is the electron-hole Coulomb interaction. In the basis of single exciton states, the Hamiltonian of the QD molecules can be expressed as

$$H_{4\times4}^{\text{eff}} = T_{4\times4}^{\text{eff}} + V_{4\times4}^{\text{eff}}, \qquad (29)$$

where

$$T_{4\times4}^{\text{eff}} = \begin{pmatrix} E_{X_{RR}} & 0 & +t_1 & -t_2 \\ 0 & E_{X_{LL}} & -t_2 & +t_1 \\ +t_1 & -t_2 & E_{X_{LR}} & 0 \\ -t_2 & +t_1 & 0 & E_{X_{RL}} \end{pmatrix} \qquad (30)$$

is the non-interacting part, and

$$V_{4\times4}^{\text{eff}} = \begin{pmatrix} 0 & V_{RRLL} & V_{RRLR} & V_{RRRL} \\ V_{RRLL}^* & 0 & V_{LLLR} & V_{LLRL} \\ V_{RRLR}^* & V_{LLLR}^* & 0 & V_{LRRL} \\ V_{RRRL}^* & V_{LLRL}^* & V_{LRRL}^* & 0 \end{pmatrix} \qquad (31)$$

is the Coulomb interaction matrix between the single exciton states.

Note that the pair of states $X_{RR}$ and $X_{LL}$ is not coupled by the single tunneling term because the scattering process between $X_{RR}$ and $X_{LL}$ requires the exchange of two particles simultaneously. For that reason this process is second order in tunneling. The same is true for the states $X_{LR}$, and $X_{RL}$.

### C. $S = 2$ bi-exciton

With increasing magnetic fields, a higher polarized state with $S = 2$, ($S_L = 1, S_R = 1$) equivalent to a bi-excitonic state tends to appear as ground-state. A bi-exciton is constructed by removing a pair of electrons from occupied states and putting into unoccupied states

$$|X_{j\to i, k\to l}\rangle = d_i^\dagger d_l^\dagger d_j d_k |\nu = 2\rangle. \qquad (32)$$

The energy of biexcitonic state can be decomposed into the energy of two single excitons plus their interaction

$$\Delta E_{XX_{j\to i, k\to l}} = \Delta E_{X_{j\to i}} + \Delta E_{X_{k\to l}} + \delta V. \qquad (33)$$

$\delta V$ is the binding energy between two excitons, accounted for the electron-electron, electron-hole and hole-hole interactions

$$\begin{aligned}
\delta V &= \langle l, i|V|i, l\rangle - \langle l, i|V|l, i\rangle \\
&\quad - \langle l, j|V|j, l\rangle \\
&\quad - \langle k, i|V|i, k\rangle \\
&\quad + \langle j, k|V|k, j\rangle - \langle j, k|V|j, k\rangle \qquad (34)
\end{aligned}$$

In the quantum dot molecule considered in this study, we find $\delta V < 0$ for large magnetic fields, i.e., two isolated excitons favor to pair and form a biexcitonic state where the energy of a biexciton is lower than energy of two isolated single excitons.
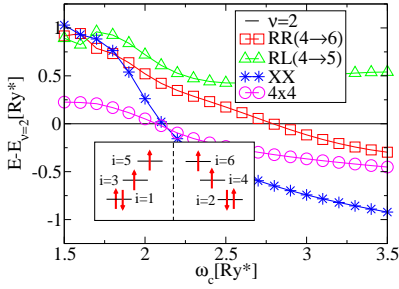
Phys. Rev. B **70**, 045324 (2004).

[12] J. J. Palacios and P. Hawrylak, Phys. Rev. B **51**, 1769 (1995).

[13] A. Galindo and M. A. Martin-Delgado, Rev. Mod. Phys. **74**, 347 (2002).

[14] J. A. Brum, and P. Hawrylak, Superlattices Microstruct. **22**, 431 (1997).

[15] D. Loss and D.P. DiVincenzo, Phys. Rev. A **57**, 120 (1998); G. Burkard, D. Loss and D. P. DiVincenzo, Phys. Rev. B **59**, 2070 (1999).

[16] Xuedong Hu and S. Das Sarma, Phys. Rev. A 64, 042312 (2001), X. Hu and S. Das Sarma, *ibid* 61, 062301 (2000).

[17] J. Kolehmainen, S.M. Reimann, M. Koskinen, M. Manninen, Eur. Phys. J. B **13**, 731 (2000).

[18] Ramin M. Abolfath, W. Dybalski, Pawel Hawrylak, Phys. Rev. B **73**, 075314 (2006).

[19] L. Martin-Moreno, L. Brey, and C. Tejedor, Phys. Rev. B **62**, R10633 (2000); David Sanchez, L. Brey, and Gloria Platero, Phys. Rev. B **64**, 235304 (2001).

[20] S. M. Girvin and A. H. MacDonald, in *Perspectives in Quantum Hall Effects: Novel Quantum Liquids in Low-Dimensional Semiconductor Structures*, edited by S. Das Sarma and A. Pinczuk (Wiley, New York, 1997).

[21] Ramin M. Abolfath, and Pawel Hawrylak, Phys. Rev. Lett. **97**, 186802 (2006).

[22] J. J. Sakurai, *Modern Quantum Mechanics*, (Addison-Wesley, 2nd Ed., 1994).

[23] Y. Nakamura, C. D. Chen, and J. S. Tsai, Phys. Rev. Lett. **79**, 2328 (1997); Y. Nakamura, Yu. A. Pashkin, and J. S. Tsai, Nature **398**, 786 (1999).

[24] James Smart, *Effective field theories of magnetism*, (Saunders, Philadelphia, 1966).

[25] S. Yamamoto, Phys. Rev. B **69**, 064426 (2004); S. Yamamoto, T. Fukui, K. Maisinger, and U. Schollwck, J. Phys.: Condens. Matter **10**, 11033 (1998); M. Abolfath, H. Hamidian, and A. Langari, cond-mat/9901063 (unpublished), and references therein.

[26] Andreas Wensauer, Marek Korkusinski, and Pawel Hawrylak, Phys. Rev. B **67**, 035325 (2003).

[27] V. W. Scarola and S. Das Sarma, Phys. Rev. A **71**, 032340 (2005).

[28] A. Szabo and N. S. Ostlund, *Modern Quantum Chemistry* (McGraw-Hill, New York, 1989).

[29] Constantine Yannouleas and Uzi Landman, Phys. Rev. B **68**, 035325 (2003); Constantine Yannouleas and Uzi Landman, Phys. Rev. B **68**, 035325 (2003); C. Yannouleas and U. Landman, J. Phys.: Condens. Matter **14**, L591 (2002); C. Yannouleas and U. Landman, Int. J. Quantum Chem. **90**, 699 (2002).

[30] M. Pioro-Ladriere, M. R. Abolfath, P. Zawadzki, J. Lapointe, S. A. Studenikin, A. S. Sachrajda, and P. Hawrylak, Phys. Rev. B **72**, 125307 (2005).

[31] Ramin M. Abolfath, and Pawel Hawrylak, J. Chem. Phys. **125**, 034707 (2006).

[32] B. D. McCombe and R. J. Wagner, Phys. Rev. B **4**, 1285 (1971).

[33] I. Žutić, J. Fabian, and S. Das Sarma, Rev. Mod. Phys. **76**, 323 (2004).